Gene 800 (2021) 145837

Contents lists available at ScienceDirect

Gene

journal homepage: www.elsevier.com/locate/gene

Research paper

Transcriptomic landscape of persistent diarrhoea in rhesus macaques and comparison with humans and mouse models with inflammatory bowel disease

Jiao Wang [a,1], Mingyi Lv [a,1], Lewei He [a], Xinqi Wang [a], Yue Lan [b], Jieyun Chen [a], Minghui Chen [a], Chunhui Zhang [b], Ruixiang Tang [a], Dan Zhou [c], Xiaoyang Deng [d], Jing Li [a], Tao Guo [e], Megan Price [a], Bisong Yue [b], Zhenxin Fan [a,b,*]

[a] Key Laboratory of Bioresources and Eco-Environment (Ministry of Education), College of Life Sciences, Sichuan University, Chengdu 610065, Sichuan, China
[b] Sichuan Key Laboratory of Conservation Biology on Endangered Wildlife, College of Life Sciences, Sichuan University, Chengdu 610064, Sichuan, China
[c] The First People's Hospital of Neijiang, Neijiang 641000, Sichuan, China
[d] Lasa Sunshine Maternity Hospital, Lasa 850000, Xizang, China
[e] Department of Obstetrics and Gynecology, West China Second University Hospital, Sichuan University, Chengdu 610041, Sichuan, China

ARTICLE INFO

Keywords:
Diarrhoea disease
human IBD
Experimental colitis
Blood transcriptome

ABSTRACT

Diarrhoea is a widespread disease in captive rhesus macaques (*Macaca mulatta*) and a small proportion of individuals may experience persistent diarrhoea. Persistent diarrhoea can lead to a compromised immune system, intestinal inflammation and malnutrition. We analyzed the blood transcriptomes of 10 persistent diarrhoeal and 12 healthy rhesus macaques to investigate the gene expression differences between the two groups. We identified 330 DEGs between persistent diarrhoeal and healthy rhesus macaques. The 211 up-regulated DEGs in the diarrhoeal group were mainly enriched in immune-related and interleukin-related categories. Among them, three interleukin (IL) 18 related DEGs (*IL18*, *IL18R1*, and *IL18BP*) played important roles in actively regulating pro-inflammatory responses. Interestingly, the up- and down-regulated DEGs were both enriched in the same immune-related categories. Thus, we applied a new method to examine the distribution of DEGs in all child categories. We found that interleukin and T cell related categories were mainly occupied by up-regulated DEGs, while immunoglobulin production and B cell related categories were enriched by down-regulated DEGs. We also compared rhesus macaque DEGs with the DEGs of inflammatory bowel disease (IBD) humans and IBD mouse models and found that 30–40% of macaque DEGs were shared with IBD humans and mouse models. In conclusion, our results showed that there were significant immune differences between persistent diarrhoeal rhesus macaques and healthy macaques, which was similar to the expression differences in IBD patients and mouse models.

1. Introduction

Diarrhoea is the second cause of mortality in children under five, and around 525, 000 children under five are killed by diarrhoeal disease each year (WHO, 2017). The cumulative effect of diarrhoea in babies and toddlers can increase the risk of stunting in 24-month-old children (Checkley et al., 2008). Acute diarrhoea is a common symptom of gastrointestinal infections caused by a host of bacterial, viral, or parasitic organisms. Most deaths of acute diarrhoea are caused by excessive fluid and electrolyte losses (Tormo et al., 2008). The common etiological agents of diarrhoeal disease include Rotavirus, *Escherichia coli*, Shigella, *Vibrio cholerae*, and *Clostridioides difficile* (WHO, 2017; Troeger et al., 2018; Oksi et al., 2019). When acute diarrhoea persists for more than 14 days, it is termed as persistent diarrhoea, the result of complex enteric

Abbreviations: IBD, inflammatory bowel disease; ICD, idiopathic chronic diarrhea; CD, Crohn's disease (CD); UC, ulcerative colitis; IL, interleukin; DEG, differentially expressed gene; GO, Gene ontology (GO); KEGG, Kyoto Encyclopedia of Genes and Genomes.

* Corresponding author at: Key Laboratory of Bioresources and Eco-Environment (Ministry of Education), College of Life Sciences, Sichuan University, Chengdu 610065, Sichuan, China.
E-mail address: zxfan@scu.edu.cn (Z. Fan).

[1] Contributed equally to this work.

https://doi.org/10.1016/j.gene.2021.145837
Received 7 March 2021; Received in revised form 26 May 2021; Accepted 13 July 2021
Available online 16 July 2021

infections (Guarino et al., 2014; Shankar and Rosenbaum, 2020). Persistent diarrhoea can lead to mucosal injury, and then result in a vicious cycle of further diarrhoea, malnutrition, and infections (Shankar and Rosenbaum, 2020).

Similar to humans, diarrhoea is a widespread disease within captive rhesus macaques (*Macaca mulatta*) (Rhoades et al., 2019), with some captive populations having more than 15–39% incidences per year (Prongay et al., 2013). Diarrhoea can greatly impact the health of rhesus macaques, causing malnutrition, growth retardation and even death (Haertel et al., 2018). The pathogens that cause diarrhoea in humans, such as Rotavirus, are also associated with diarrhoea in rhesus macaques (Wang et al., 2019). Acute diarrhoea in rhesus macaque can be treated successfully given appropriate diagnosis and treatment. However, a small proportion of diarrhoeal disease in rhesus macaques can become persistent and recurrent diarrhoea (e.g. diopathic chronic diarrhoea (ICD)) (Wang et al., 2019; Westreich et al., 2019; Ardeshir et al., 2013). The typical symptoms of ICD are repeated episodes of intestinal distress and inflammation but without clearly known pathogens (Ardeshir et al., 2013; Broadhurst et al., 2012). Persistent and recurrent diarrhoea (e.g. ICD) is the main cause of morbidity and mortality in young captive macaques (Wang et al., 2019; Westreich et al., 2019; Ardeshir et al., 2013).

The phenotype of ICD in rhesus macaques is very similar to inflammatory bowel disease (IBD) in humans (Westreich et al., 2019). IBD is a chronic, inflammatory disease in the gastrointestinal tract, broadly divided into Crohn's disease (CD) and ulcerative colitis (UC). IBD has a complex etiology and is difficult to treat, and is often accompanied by a clinical manifestation of persistent diarrhoea (Anbazhagan et al., 2018). The mechanism associated with diarrhoea in IBD is predominantly impaired ion transport and loss of epithelial barrier function (Anbazhagan et al., 2018). The incidence of IBD has increased in the past few decades and therefore investigators have turned considerable attention to exploring the pathogenesis and treatment of IBD (Anbazhagan et al., 2018; Wędrychowicz et al., 2016; Jeong et al., 2019).

Considering the close relationship to humans (Gibbs et al., 2007; Lan et al., 2020; Zhou et al., 2020) and symptom similarities between persistent diarrhoea in rhesus macaques and human IBD, it is possible that persistent diarrhoea in rhesus macaques has similar physiological causes to human IBD. Consequently, human-macaque gene expression profiles may similarly change between healthy and diarrhoeal individuals. To test this hypothesis, we sequenced the blood transcriptomes of 10 rhesus macaques with persistent and recurrent diarrhoea and 12 healthy control individuals from the same captive population with RNA-seq technology. We aimed to identify the transcriptomic landscape of persistent diarrhoea in rhesus macaques, to detect the gene expression changes between unhealthy and healthy individuals, and to assess the molecular pathways and networks that are related to persistent diarrhoea. Furthermore, we compared the gene expression profiles among persistent diarrhoeal rhesus macaques, human IBD patients, and IBD mouse models, to explore the similarities of differentially expressed genes (DEGs) and molecular pathways. The findings of this study provide a foundation for better understanding the genetic mechanisms and pathophysiology of persistent diarrhoea in rhesus macaques, and to aid in identifying new diagnostic and therapeutic targets.

2. Results

2.1. Data collection and transcriptome assembly

We collected samples from 10 rhesus macaques with persistent diarrhoea and 12 healthy (control) individuals. Considering the influence of sex and age, our individuals included both males and females, as well as young and adult rhesus macaques in both persistent diarrhoeal and healthy groups (Table S1). In total, we obtained 280.84 billion 150 bp paired-end clean reads. All clean reads were aligned to the reference genome (*M. mulatta,* Mmul_10) with an average mapping rate of 95.38%. We then performed a hierarchical cluster analysis, based on inter-array correlation. The results showed distinct clustering of persistent diarrhoeal and healthy groups (Fig. S1).

2.2. DEGs between persistent diarrhoeal and healthy rhesus macaques

Next, we processed all the samples with the same bioinformatics pipeline to identify DEGs between persistent diarrhoeal and healthy rhesus macaques. We identified 330 genes as DEGs between persistent diarrhoeal and healthy rhesus macaques. Of these 330, 65 had a greater than 2-fold change (Table S2, Fig. S2). Compared to healthy macaques, 211 DEGs were up-regulated in the persistent diarrhoeal group, and the remaining 119 DEGs were down-regulated. We have tabulated the DEGs with log2 fold change $\geq$ 3 in Table 1 to highlight major differences between healthy and persistent diarrhoeal individuals. The CC chemokine ligand 23 (*CCL23*), from a chemokine superfamily, had the highest log2 fold change value (5.64) in the up-regulated group and is a protein involved in immunoregulatory and inflammatory processes (Simats et al., 2018). The gene *LY6D,* a member of the lymphocyte antigen 6 family, had the highest log2 fold change within the down-regulated DEGs in persistent diarrhoeal macaques. Noteworthy, we identified three IL-18-related up-regulated DEGs (*IL18*, *IL18R1*, and *IL18BP*) in persistent diarrhoeal rhesus macaques, which play important roles in immune response process.

2.3. Enrichment analyses of DEGs showed significant immune-related changes

We performed Gene Ontology (GO) category and Kyoto Encyclopedia of Genes and Genomes (KEGG) pathway enrichment analyses of the up- and down-regulated DEGs to better understand the biological roles of the DEGs (Tables S3, S4). Only three and five pathways in the KEGG analysis were enriched in up- and down-regulated DEGs, respectively (Tables S3, S4). Up-regulated DEGs from the persistent diarrhoeal group were mainly enriched in immune-related GO categories, such as immune response (GO:0006955), innate immune response (GO:0045087), and immune system process (GO:0002376) (Fig. 1A, Table S3). We also found persistent diarrhoeal group up-regulated DEGs enriched in several interleukin-related categories, for example, interleukin-18 binding (GO:0042007), interleukin-1 production (GO:0032612), and regulation of interleukin-1 production (GO:0032652). Other categories that may be associated with diarrhoeal disease, such as cytokine production (GO:0001816), chemokine receptor binding (GO:0042379), and defense response (GO:0006952), were also enriched. Down-regulated DEGs of the persistent diarrhoeal group were enriched in categories related to the cell, including multicellular organismal process (GO:0032501), cell motility (GO:0048870), and cell migration (GO:0016477). Unexpectedly, up-regulated and down-regulated DEGs were enriched in the immune response and immune system process categories, (Fig. 1B, Table S4). In addition, DEGs were enriched in several other immune-related categories, such as immunoglobulin production (GO:0002377), lymphocyte activation (GO:0046649), and leukocyte activation (GO:0045321).

Since we mainly found immune-related GO categories, we selected both enriched and non-enriched categories to illustrate the percentage of up- and down-regulated DEGs within each of the immune-related GO categories (Fig. 1C, Table S5). All of these immune-related categories had low proportions of DEGs (<10%). However, it was clear that nearly all the categories had higher proportions of DEGs in the diarrhoeal group than the healthy group, especially the interleukin-related categories. Whereas a few categories, such as immunoglobulin production and B cell activation, had higher proportions of DEGs in the healthy group (Fig. 1C). We also found DEGs that were not enriched in several important immune-related categories (e.g. inflammatory response, T cell activation, humoral immune response), but were still associated

Table 1
The DEGs with log2 fold change ≥ 3. "padj" means adjusted P value.

Ensembl ID	Gene name	Description	log2FoldChange	padj	Up/down in diarrhoeal group
ENSMMUG00000002467	*CCL23*	chemokine (C–C motif) ligand 23	5.643250	0.001513	up
ENSMMUG00000053857	*CXHXorf48*	Chromosome X open reading frame 48	5.532995	0.028394	up
ENSMMUG00000001467	*COL1A1*	collagen type I alpha 1 chain	4.603902	0.013828	up
ENSMMUG00000039654	*COL1A2*	collagen type I alpha 2 chain	4.445696	0.026659	up
ENSMMUG00000016831	*DGKI*	diacylglycerol kinase iota	3.570314	0.020676	up
ENSMMUG00000064811	ENSMMUG00000064811	None	3.479227	0.000701	up
ENSMMUG00000004489	*MMP8*	matrix metallopeptidase 8	3.431662	0.005664	up
ENSMMUG00000016838	*CHD5*	chromodomain helicase DNA binding protein 5	3.384416	0.013256	up
ENSMMUG00000020930	ENSMMUG00000020930	receptor accessory protein 1	3.247237	0.000570	up
ENSMMUG00000002742	*ST8SIA5*	ST8 alpha-N-acetyl-neuraminide alpha-2,8-sialyltransferase 5	3.240552	0.001212	up
ENSMMUG00000004177	*MYO7B*	myosin VIIB	3.054862	0.011109	up
ENSMMUG00000051619	*PADI3*	peptidyl arginine deiminase 3	−3.093264	0.040161	down
ENSMMUG00000054865	ENSMMUG00000054865	None	−3.269539	0.000382	down
ENSMMUG00000022615	*EGFL6*	EGF like domain multiple 6	−3.355761	0.028538	down
ENSMMUG00000007504	*MYO5C*	myosin VC	−3.447986	0.001735	down
ENSMMUG00000021783	*IGDCC3*	immunoglobulin superfamily DCC subclass member 3	−3.642991	0.000255	down
ENSMMUG00000018057	*UMODL1*	uromodulin like 1	−3.677965	0.010711	down
ENSMMUG00000015427	*FSCN3*	fascin actin-bundling protein 3	−5.571815	0.001878	down
ENSMMUG00000060008	*LY6D*	lymphocyte antigen 6 family member D	−5.612746	0.000013	down

with the categories (Fig. 1C, Table S5).

2.4. DEG flow in immune-related GO trees

There were 59 up- and down-regulated DEGs (36 up, 23 down) (Table S6) DEGs enriched in two immune-related categories, immune response (GO:0006955) and immune system process (GO:0002376). These 59 DEGs accounted for 17.88% of the total number of DEGs. Therefore, we created a new way to investigate distribution differences between 59 up- and down-regulated DEGs and associated immune response, immune system process and child categories. We first illustrated the main child categories of the immune system process (GO:0002376) because it is an ancestor category of immune response (GO:0006955) (Fig. 1D, Table S7). All 59 up- and down-regulated DEGs were found in the immune system process category, and mainly flowed into the categories of immune response (GO:0006955), regulation of immune system process (GO:0002682), and leukocyte activation (GO:0045321) (Fig. 1D). Most categories within the immune system process hierarchy were associated with higher numbers of up-regulated DEGs, while only three of the categories had more numbers of down-regulated DEGs.

We then illustrated a more detailed DEG distribution in the child categories of immune response (GO:0006955) and leukocyte activation (GO:0045321). We observed the different flow directions of the up- and down-regulated DEGs in the child categories of immune response (Fig. 2A, Table S8). Although the immune response was enriched by both up- and down-regulated DEGs, the up-regulated DEGs occupied most of the child categories (pink), such as GO:0045088 (regulation of innate immune response), GO:0002228 (natural killer cell mediated immunity), and GO:0002460 (adaptive immune response based on somatic recombination of immune receptors built from immunoglobulin superfamily domains). Down-regulated DEGs were only distributed in small numbers in the child categories, and they finally flowed to GO:0002757 (immune response-activating signal transduction) and GO:0002278 (eosinophil activation involved in immune response). In the leukocyte activation category, which was only enriched by down-regulated DEGs, up- and down-regulated DEGs showed different flow directions (Fig. 2B, Table S9). The up-regulated DEGs finally flowed to several T cell related categories, including GO:0030217 (T cell differentiation) and GO:0046631 (alpha-beta T cell activation) (e.g. *SOCS1, CLEC4A, IL18R1, IL18, IFNG, LAG3*, and *EGR1*). Whereas the down-regulated DEGs mainly flowed to B cell related categories GO:0042113 (B cell activation), and GO:0030183 (B cell differentiation) (e.g. *CD79A, CD79B, MS4A1, BANK1,* and *TNFRSF13B*).

Furthermore, we illustrated the distribution of DEGs in defense response (GO:0006952) and is also related to the immune system (Fig. S3, Table S10). We found that there were 25 up-regulated DEGs and only 5 down-regulated DEGs associated with this defense response GO category. The two immune-related categories, innate immune response (GO:0045087) and inflammatory response (GO:0006954), had more than 10 up-regulated DEGs but only had two or three down-regulated DEGs in each of them (Fig. S3).

2.5. Comparison between macaques, IBD humans, and IBD mouse models

We compared our macaque DEGs with the DEGs of IBD humans and mice to better understand the similarities and differences between persistent diarrhoea in rhesus macaques and IBD. We collected the DEGs between IBD humans and healthy controls, and the DEGs between IBD model mice and wild-type mice from previous publications (Table 2). We obtained 321 DEGs from human whole blood and 2645 from human intestines (Table S11). In mice, we found 4415 DEGs in intestines (Table S11) after transforming them into human lineal homologous genes. Similarly, we obtained 270 human lineal homologous genes from our rhesus macaque DEGs (Table S11).

We compared the DEGs among the following four groups: rhesus macaque, human blood, human intestines, and mouse intestines. We obtained the numbers of overlapping DEGs between groups (Fig. 3A, Table S12). There were only five commonly shared DEGs in all four groups. There were 17, 75, and 109 overlapping DEGs in paired comparisons of rhesus macaque vs human blood, rhesus macaque vs human intestines, and rhesus macaque vs mouse, respectively.

Next, we calculated the percentage of overlapping DEGs in each paired comparison. We did this by dividing the numbers of overlapping DEGs by the total number of rhesus macaque DEGs (Fig. 3B, right panel). The highest percentage of overlapping DEGs was between the rhesus macaque and mouse, accounting for 40.37% of macaque DEGs (Fig. 3B, right panel). Opposite to our expectations, the percentage of overlapping DEGs between rhesus macaque and human blood tissue was the lowest, only 6.30%, yet the DEGs were from the same tissue type. The low percentage overlap could have been due to the number of DEGs in the dataset. The human blood dataset only contained 321 DEGs, which was 8X less than the human intestines dataset and 13X less than the mouse. Therefore, we divided the numbers of overlapping DEGs by the sum of the two groups' DEGs in each comparison (Fig. 3B, left panel) to eliminate the influence of gene number differences between groups.

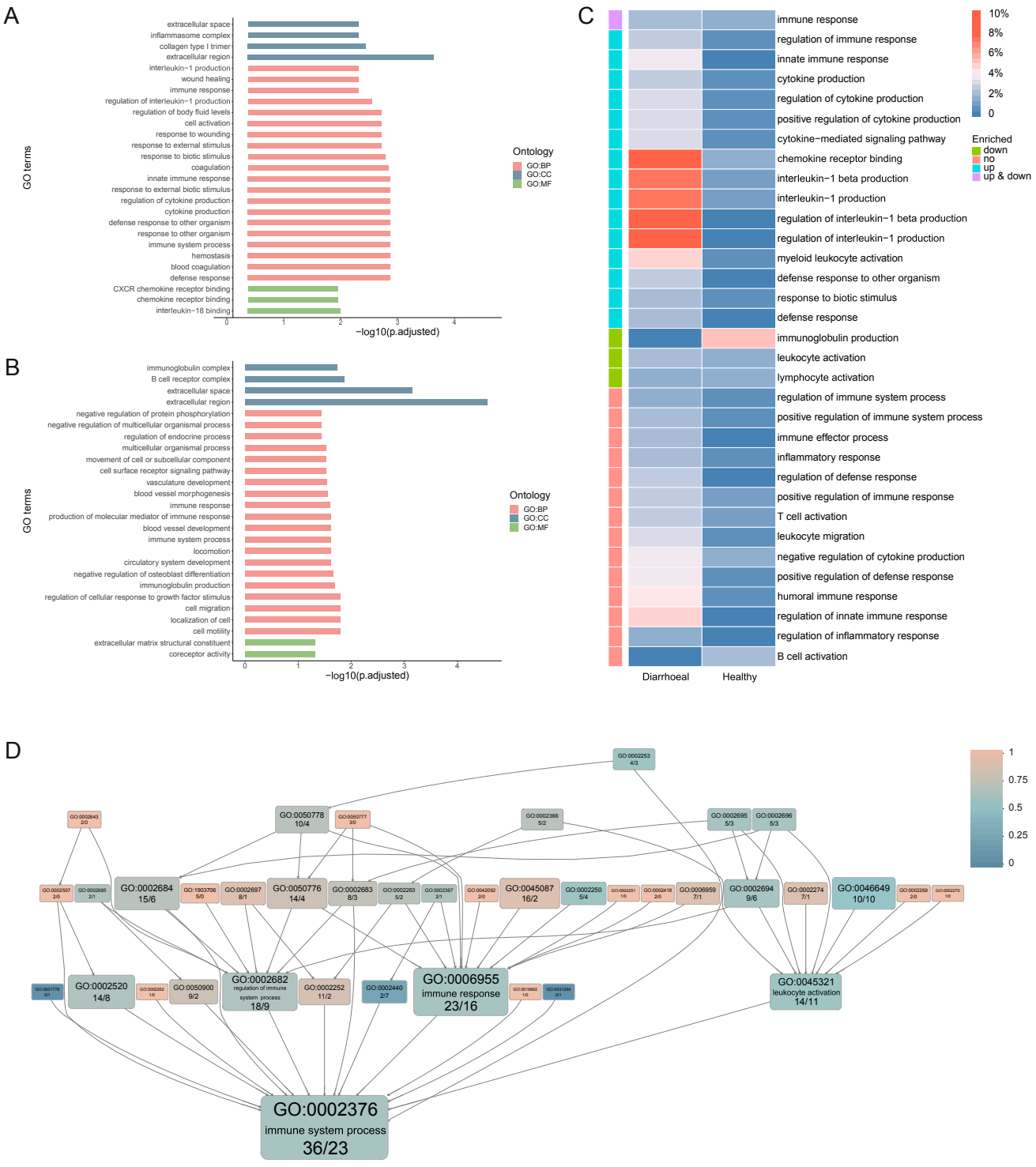

Fig. 1. The DEGs between persistent diarrhoeal and heathy control rhesus macaques. A. The GO enrichment analysis of up-regulated DEGs in persistent diarrhoeal rhesus macaques. B. The GO enrichment results of down-regulated DEGs in persistent diarrhoeal rhesus macaques. C. The heatmap of DEG percentages in selected immune-related GO categories with both enriched and non-enriched. D. The GO tree of 59 immune-related DEGs in immune system process. The box numbers represented the up- (front) and down-regulated (behind) DEGs, and the size of box represented the relative amount of DEG in the category. The box colour equated to the numbers of up-/down-regulated DEGs, with up-regulated represented by pink and down-regulated equalling blue. (For interpretation of the references to colour in this figure legend, the reader is referred to the web version of this article.)

Subsequently, the differences in the percentages of overlapping DEGs in paired comparisons were small. The highest percentage of overlapping DEGs was between rhesus macaque and human blood (2.88%), while rhesus macaque and mouse had the lowest (2.33%). The same tissues (rhesus macaque and human blood) and the more closely related species (rhesus macaque and human) had a higher proportion of overlapping DEGs (Fig. 3B, left panel). Most of the overlapping DEGs between rhesus macaque and different human datasets were up-regulated regardless of accounting for dataset size. However, the majority of overlapping DEGs between rhesus macaque and mouse were down-regulated.

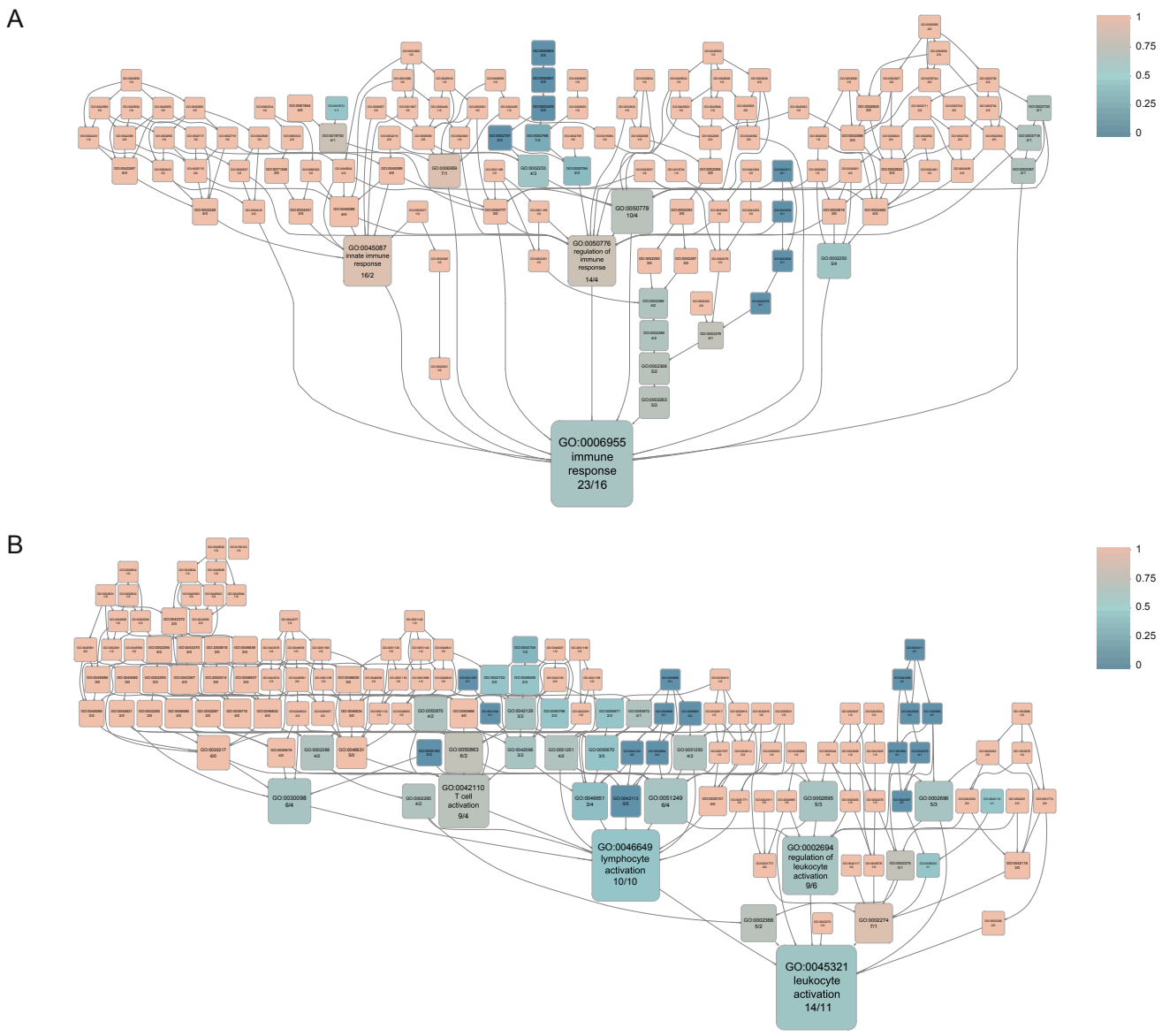

Fig. 2. The DEGs distribution within GO trees in the child categories of immune response (GO:0006955) and leukocyte activation (GO:0045321). A. The GO tree of the immune response (GO:0006955). B. The GO tree of leukocyte activation (GO:0045321). The explanations of box numbers and colour were same to Fig. 1D.

We then focused on the gene expression of the above overlapping DEGs. In total, we obtained 147 overlapping DEGs from the three species after retransformation into rhesus macaque lineal homologous genes (Table S13). The gene expression heatmap of those overlapping DEGs clearly clustered into two groups (diarrhoeal group and healthy group) and showed significant expression differences (Fig. 3C). The GO enrichment analysis demonstrated that the DEGs were also enriched in many immune-related categories (Fig. 3D, Table S14).

3. Discussion

Persistent diarrhoea can lead to a compromised immune system, intestinal inflammation, and even malnutrition (Checkley et al., 2008; Bandsma et al., 2019). As the first study investigating the transcriptomic landscape of persistent diarrhoeal rhesus macaques, we analyzed the gene expression changes of persistent diarrhoea in rhesus macaques. We observed that the major differences between persistent diarrhoeal rhesus macaques and healthy individuals were associated with immune-related genes and pathways. Previously, adequate explanations of why some GO categories were enriched by both up- and down-regulated DEGs was lacking. Additionally, most investigations had only focused on enriched GO categories, but detailed information regarding their child levels and related categories was missing. Here, we uniquely analyzed the distribution of DEGs in several important immune-related GO categories and all of their child categories (Fig. 1D, Fig. 2, and Fig. S3). Consequently, we examined whether the up- and down-regulated DEGs actually flowed into different child categories.

The immune system process GO category had 59 DEGs and a large proportion of them flowed to the immune response category (Fig. 1D). The immune response was enriched in 23 up-regulated DEGs and 16 down-regulated DEGs (Fig. 2A). We observed that 16 of the 23 up-regulated DEGs flowed to the innate immune response category, which only contained 2 down-regulated DEGs. Moreover, we investigated other important immune-related GO categories, such as leukocyte activation (Fig. 2B) and defense response (Fig. S3). Interestingly, although leukocyte activation was only enriched by down-regulated DEGs, there were more up-regulated DEGs within it. Its child category, lymphocyte activation, had 10 up- and 10 down-regulated DEGs. Lymphocyte activation's up-regulated DEGs mainly flowed to T cell related child categories, whereas the down-regulated DEGs mainly

Table 2
The details of previous investigations, from which we collected the DEGs between IBD humans and healthy controls, and the DEGs between IBD mouse modes and wild-type mouse.

Species	Tissue	Group	Technology	Reference
Human	Whole blood	Active UC vs Healthy Controls	microarray	PMID: 28,981,629
Human	Whole blood	Active CD or UC_vs_Healthy Concrols	RNA-seq	PMID: 30541017
Human	Whole blood	Active CD or UC_vs_Healthy Concrols	RNA-seq	PMID: 30541017
Human	intestinal mucosa	UC vs Healthy Controls	RNA-seq	PMID: 32016358
Human	intestinal mucosa	CD vs Healthy Controls	microarray	PMID: 17262812
Human	intestinal mucosa	UC vs Healthy Controls	microarray	PMID: 17262812
Human	intestinal mucosa	UC vs Healthy Controls	microarray	PMID: 18523026
Human	intestinal mucosa	Inflamed mucosa of CD vs Healthy Controls	RNA-seq	PMID: 28613228
Human	intestinal mucosa	Non-Inflamed mucosa of CD vs Healthy Controls	RNA-seq	PMID: 28613228
Human	intestinal mucosa	CD vs Healthy Controls	microarray	PMID: 24108111
Human	intestinal mucosa	only-colon-CD vs Healthy Control	RNA-seq	PMID: 25003194
Human	intestinal mucosa	UC vs Healthy Contorl	RNA-seq	PMID: 25003194
Human	intestinal mucosa	UC vs Healthy Controls	RNA-seq	PMID: 29040430
Human	colon biopsies	CD vs Healthy Controls	RNA-seq	PMID: 25795566
Human	colon biopsies	UC vs Healthy Controls	RNA-seq	PMID: 25795566
Mouse	cecal	IL10-deficient with colitis vs Healthy Wild-type	microarray	PMID: 19133689
Mouse	colon	AdTr model vs BALB/c Wild-type	RNA-seq	PMID: 25795566
Mouse	colon	DSS model vs BALB/c Wild-type	RNA-seq	PMID: 25795566
Mouse	colon	PAC IL-10 k.o. model vs C57BL/6J Wild-type	RNA-seq	PMID: 25795566
Mouse	colon	DSS vs Healthy Controls	RNA-seq	PMID: 29773794
Mouse	colon	DSS + ER-464195–01 vs Healthy Controls	RNA-seq	PMID: 29773794
Mouse	ileum	Intestinal schistosomiasis inflammation vs Healthy Controls	microarray	PMID: 22,866,923
Mouse	ileum	TNBS-induced ileitis inflammation vs Healthy Controls	microarray	PMID: 22,866,923
Mouse	colon	CD45RB Transfer vs Healthy Controls	microarray	PMID: 17,206,675
Mouse	colon	DSS vs Healthy Controls	microarray	PMID: 17,206,675
Mouse	colon	TNBS vs Healthy Controls	microarray	PMID: 17,206,675

flowed to B cell related child categories. T cells were the key mediators in cell-mediated immunity, and B cells were the key mediators in humoral immunity. The distribution differences of the up- and down-regulated DEGs in lymphocyte activation indicated the persistent diarrhoeal group and the healthy group probably differed in their cell-mediated immunity and humoral immunity. Consequently, based on this method, we clearly observed that the up-regulated DEGs had prominent frequency in most of the child levels within the investigated immune-related GO categories regardless of whether they were enriched by the down-regulated DEGs. The flow directions of the up- and down-regulated DEGs also exhibited significant differences, which reflected the possible functional differences between diarrhoeal and healthy individuals.

Several genes have been reported as being associated with diarrhoea and immune changes. For example, interleukin (IL) plays important roles in human IBD, including IL-10, IL-12, IL-17, IL-18, and IL-33 (Moschen et al., 2019; Magyari et al., 2014; Su and Zhao, 2020; Williams et al., 2019). We identified three IL-18-related up-regulated DEGs (*IL18*; *IL18R1*, and *IL18BP*) in persistent diarrhoeal rhesus macaques (Table S2). We also found several enriched IL-related GO categories associated with up-regulated DEGs, such as interleukin-18 binding (GO:0042007) and interleukin-1 production (GO:0032612) (Fig. 1A, Table S3). IL-18 plays an important role in actively regulating pro-inflammatory responses in intestinal diseases, such as IBD (Williams et al., 2019). In clinical investigations, increased epithelial secretion IL-18 was correlated with increased severity of IBD (Pizarro et al., 1999). Our findings were consistent with previous investigations in humans, showing that the persistent diarrhoeal rhesus macaques experienced similarly inflammation with IBD.

Immunoglobulin, one of the immunoreactive molecules, can protect the body from pathogenic bacteria and viruses. We found six down-regulated DEGs enriched in the immunoglobulin production (GO:0002377) category but lacking any up-regulated DEGs (Fig. 1B, Table S4). Low immunoglobulin G (IgG) levels have often been observed in IBD patients in clinical investigations (Rai et al., 2015) and low IgG levels are associated with poor clinical outcomes in IBD patients (Rai et al., 2015; Horton et al., 2016). Therefore, administration of intravenous immunoglobulin is beneficial in patients with medically refractory IBD (Horton et al., 2017; Merkley et al., 2015; Rogosnitzky et al., 2012). The low gene expression levels of immunoglobulin-related genes in persistent diarrhoeal rhesus macaques were consistent with observations in IBD patients, which suggests administering intravenous immunoglobulin to rhesus macaques with persistent diarrhoea may be beneficial. However, IgG levels in diarrhoeal and healthy rhesus macaques should be studied prior to this treatment.

The sampled diarrhoeal rhesus macaques were experiencing persistent and recurrent diarrhoea. Several macaques experienced recurrent diarrhoea for more than one year. The veterinarian did not detect any known intestinal pathogens by culture-based methods. Without biopsies and other tests, we could not determine the presence of pathogens and could not accurately diagnose the cause. Given the macaque's symptoms were very similar to ICD and IBD and their major gene expression changes were associated with immune-related genes and pathways, we believed that comparisons of DEGs in diarrhoeal rhesus macaques with IBD humans and the IBD mice model were worthwhile and necessary (Fig. 3).

Ample research associated with IBD humans and IBD mice model has been conducted. For example, researchers used hybridization-based methodologies (e.g. microarrays) and RNA-seq technology to detect the gene expression differences between IBD patients and healthy people, which was usually based on blood or colonic biopsies (Wu et al., 2007; Noble et al., 2008; Ben-Shachar et al., 2013; Planell et al., 2013; Planell et al., 2017; Holgersen et al., 2015; Hong et al., 2017; Taman et al., 2018; Ostrowski et al., 2019; Quraishi et al., 2020). In addition, different mouse models of human IBD, such as the dextran sodium sulfate (DSS) model and 2,4,6-trinitrobenzene sulfonate (TNBS)-induced model, were widely used in various human IBD research fields (Avula et al., 2012; te Velde et al., 2007; Rankin et al., 2018; Ohkuro et al., 2018; Czarnewski et al., 2019). We collected the DEGs between IBD humans and healthy controls, and the DEGs between IBD model mice and wild-type mice from those ample previous publications and compared with our results of rhesus macaque.

Our paired comparisons found that 30%~40% of the total DEGs in diarrhoeal rhesus macaques were reported in IBD patients and mouse models (Fig. 3), indicating similarities between the gene expression

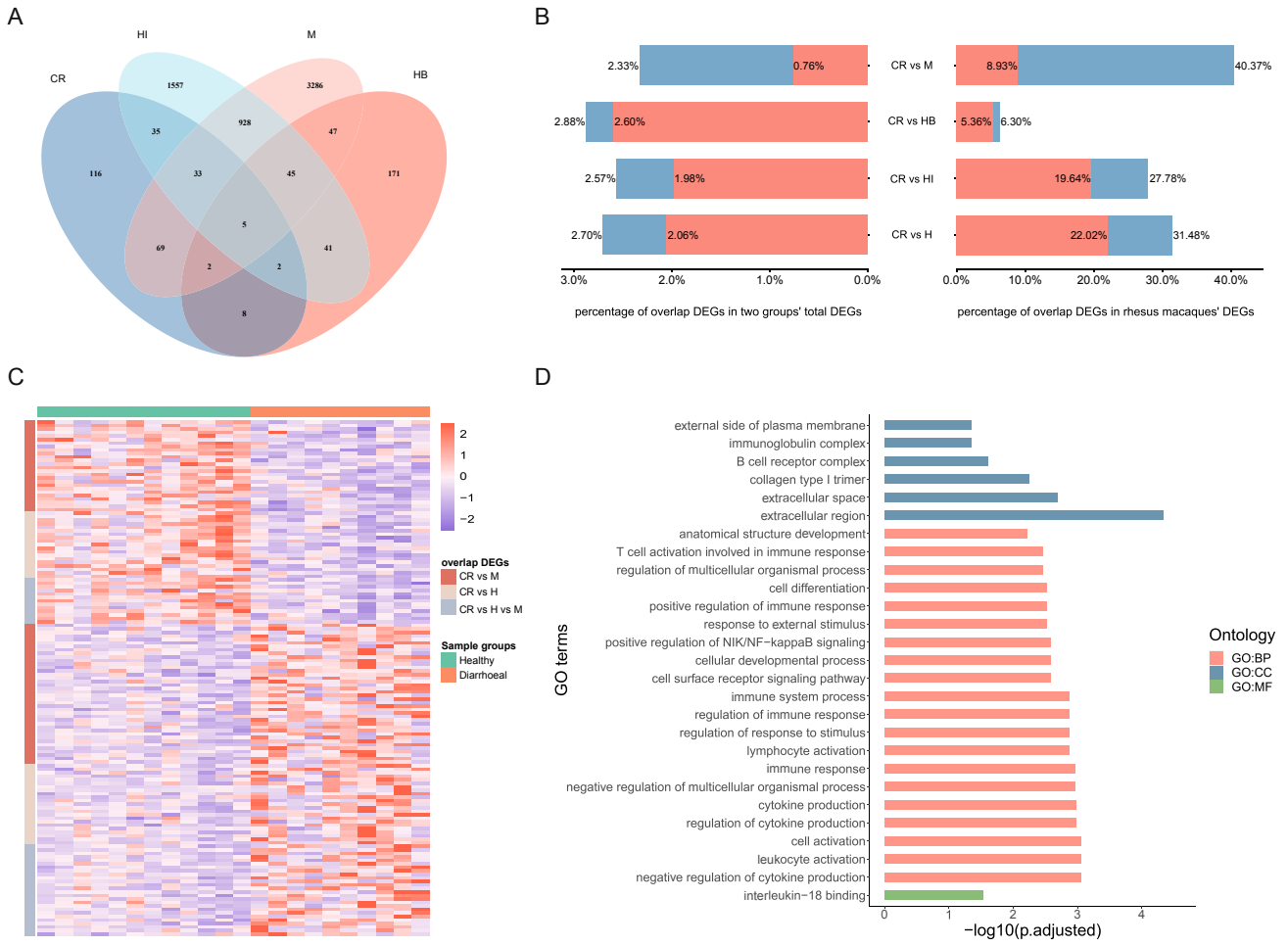

Fig. 3. The DEGs comparison of macaque, IBD human, and IBD mouse model data. A. The Venn diagram of overlapping DEGs between four groups; rhesus macaque, human blood, human intestines, and mouse intestines. B. Percentage of overlapping DEGs in rhesus macaque DEGs. Total DEGs is represented by blue and up-regulated DEGs is represented by red. C. The expression heatmap of overlapping DEGs in paired comparisons; rhesus macaque and human, and rhesus macaque and mouse. D. The GO enrichment results of overlapping DEGs in paired comparisons; rhesus macaque and human, and rhesus macaque and mouse. Acronyms are: CR = (Chinese) rhesus macaque, HI = human intestines, HB = human blood, and M = mouse. (For interpretation of the references to colour in this figure legend, the reader is referred to the web version of this article.)

profiles of the persistent diarrhoeal rhesus macaques and IBD patients and mouse models. Our findings, such as the result of GO enrichment analysis (immune-related categories) of rhesus macaque DEGs and overlapping DEGs among macaques, humans and mice, suggested that the persistent diarrhoeal rhesus macaques experienced similar inflammation and IBD-like disease to IBD patients and mouse models. Therefore, it is possible that treatments for IBD patients may be beneficial in persistent diarrhoeal rhesus macaques. In addition, persistent diarrhoeal rhesus macaques could be a potential animal model to study the genetic mechanisms and pathophysiologies of persistent and recurrent diarrhoea and IBD, especially the immune-related changes.

4. Materials and methods

4.1. Sample collection

We collected whole peripheral blood from persistent diarrhoeal and healthy captive Chinese rhesus macaques housed at the Sichuan Greenhouse Biotech Co., Ltd. in Meishan, Sichuan, China, to determine gene expression changes in diarrhoeal individuals. Captive macaques were housed in the same conditions and fed the same diet. We minimized sex and age effects by selecting differently aged individuals and both sexes (Table S1). The blood samples were grouped according to individuals being ± diarrhoea, with 10 persistent diarrhoeal macaques and 12 healthy macaques. The diarrhoeal rhesus macaques were characterized as having long-term, recurrent and persistent diarrhea and no response to antibiotics treatment. The asymptomatic controls had not presented with diarrhoeal symptoms 30 days prior to sampling. The diarrhoeal macaques had been treated frequently using antibiotics including levofloxacin, metronidazole, cephalosporin, gentamycin, and florfenicol, but the experimental macaques did not receive antibiotics 30 days prior to sample collection.

PAXgene Blood RNA tubes were used to collect fresh blood samples. The samples were first stored at room temperature (about 18–20 °C) for four hours, and then transferred to −20 °C for 24 h. Finally, we preserved all blood samples at −80 °C until RNA extraction. Our samples were sent to Novogene (Beijing, China) for sequencing with Illumina NovaSeq 6000 with a paired-end sequencing length of 150 bp (PE150). This study was approved by the Ethics Committee of College of Life Sciences, Sichuan University (No. 20200529001). We strictly obeyed the guidelines of the management committee of experimental animals of Sichuan Province, China (SYXK-Sichuan, 2019-192) in the sample collection and utility protocols.

4.2. Library preparation and RNA sequencing

A total of 3 μg RNA per blood sample was used as input material for RNA sample preparations. Sequencing followed the manufacturer's

PAXgene Blood RNA kit manual to extract total RNA, and used an Agilent 2100 Bioanalyzer (Agilent Technologies, Santa Clara, CA) to assess RNA quality. Total RNA was processed with the GlobinZero kit (Epicentre, Illumina, Madison, WI) and purified with a modified Qiagen RNeasy MinElute (Qiagen Inc., Valencia, CA) cleanup procedure or ethanol precipitation. Samples with RIN (RNA integrity number) values higher than 7.5 were used for library construction and sequencing, following the manufacturer's instructions. Sequencing used the Illumina NovaSeq 6000 for all of the libraries with a paired-end sequencing length of 150 bp (PE150).

4.3. Read alignment and quality control

We obtained the high-quality reads using NGS QC Toolkit v2.3.3 (Patel et al., 2012) with the same criteria used in our previous investigation (Tang et al., 2020), with stringent criteria (high-quality paired reads with more than 90% of bases with Q-value $\geq$ 30 were retained) to remove the low-quality paired-end reads or reads containing adaptors. We then mapped the processed reads to the reference genome (*M. mulatta,* Mmul_10) using HISAT2 v2.1.0 (Kim et al., 2015). We assembled transcriptomes and obtained raw read counts for each gene and transcript using StringTie v1.3.6 (Pertea et al., 2015). Finally, we obtained the expression value of TPM (transcripts per million) and raw read counts for each gene and transcript using a reference annotation file. We downloaded the genome sequences and annotations from Ensembl release-98 (www.ensembl.org).

4.4. Gene cluster analysis, identification of DEGs and enrichment analyses

We used agglomerative hierarchical clustering in the ComplexHeatmap R package (Gu et al., 2016) to perform a cluster analysis. The R package DESeq2 (Love et al., 2014) was used to identify the differentially expressed genes (DEGs) between the two groups; persistent diarrhoeal and healthy groups. We corrected all statistical test results for multiple testing with the Benjamini-Hochberg false discovery rate (FDR $\leq$ 0.05) and determined the significant differences in gene expression with an absolute value of log2 fold change $\geq$ 1. Furthermore, we performed GO and KEGG enrichment analyses using g:Profiler (Raudvere et al., 2019) to determine the biological function of the DEGs in rhesus macaques. We plotted the bar charts of the GO enrichment analysis using R package ggplot2 (version 3.3.3) (Wickham, 2106), selecting the top 20 categories of each GO class.

We obtained the total gene number in each GO category using R package gprofiler2 (version 0.2.0) (Raudvere et al., 2019) and plotted the heatmap of DEG percentages in GO categories. Our criteria for selecting the GO categories to be plotted in the heatmap were: 1) we prioritized the categories that were enriched in both up- and down-regulated genes; 2) we selected enriched immune-related categories; 3) we selected several DEGs from immune-related categories that were not enriched; 4) we excluded categories that had less than five up- or down-regulated DEGs.

4.5. DEG flow in immune-related GO trees

The hierarchical relationships between GO categories in GO trees were obtained using the R package GO.db (version 3.10.0). We investigated the distribution of 59 DEGs within the immune system process GO tree and its enriched child categories. We then selected three child categories (GO:0006955, GO:0002682, and GO:0045321) that had the most abundant DEGs and illustrated the distribution of their DEGs (Fig. 1D). Any child categories with no DEGs were deleted. Additionally, we illustrated the distribution of DEGs in the GO trees, GO:0006955 (Fig. 2A), GO:0045321 (Fig. 2B), and GO:0006952 (Fig. S3). We mapped to the lowest level of child category within these three trees, but excluded child categories with no DEGs.

4.6. Data of IBD patients and mouse models

We collected the DEGs from previously studied IBD humans and IBD mouse models. The groups we selected were all IBD vs healthy controls. We transformed the lineal homologous genes by the Ensembl BioMart tool. The overlapping heatmap of the three species' DEGs (i.e. macaque, human, mouse) was plotted by the ComplexHeatmap R package (Gu et al., 2016). The GO enrichment analysis used g:Profiler (Raudvere et al., 2019), and plotted bar charts using ggplot2 (version 3.3.3) (Wickham, 2106).

Declaration of Competing Interest

The authors declare that they have no known competing financial interests or personal relationships that could have appeared to influence the work reported in this paper.

Acknowledgements

This work was supported by the National Natural Science Foundation of China (32070413) and Sichuan Science and Technology Program (2020YJ0303). We thank Mr. Guanglun Lei at Sichuan Green-house Biotech Co., Ltd for sample collection.

Author Statement

Jiao Wang, Mingyi Lv, Leiwei He, Xinqi Wang, Yue Lan and Chunhui Zhang performed the bioinformatics analyses and collected the samples; Ruixiang Tang, Minghui Chen, Dan Zhou and Xiaoyang Deng performed the experiments; Jiao Wang wrote the manuscript; Tao Guo, Megan Price, Bisong Yue, Jing Li and Zhenxin Fan revised the manuscript; Zhenxin Fan designed and supervised the study.

Availability of Data

The raw sequencing reads from this study have been submitted to CNGBdb (https://db.cngb.org/cnsa/) with Project number CNP0001564 and NCBI BioProject with number PRJNA628554. Details can be found in Table S1.

Appendix A. Supplementary data

Supplementary data to this article can be found online at https://doi.org/10.1016/j.gene.2021.145837.

References

Anbazhagan, A.N., Priyamvada, S., Alrefai, W.A., Dudeja, P.K., 2018. Pathophysiology of IBD associated diarrhea. Tissue Barriers. 6 (2), e1463897. https://doi.org/10.1080/21688370.2018.1463897.

Ardeshir, A., Oslund, K.L., Ventimiglia, F., Yee, J., Lerche, N.W., Hyde, D.M., 2013. Idiopathic microscopic colitis of rhesus macaques: quantitative assessment of colonic mucosa. Anat. Rec. (Hoboken) 296 (8), 1169–1179. https://doi.org/10.1002/ar.22727.

Avula, L.R., Knapen, D., Buckinx, R., et al., 2012. Whole-genome microarray analysis and functional characterization reveal distinct gene expression profiles and patterns in two mouse models of ileal inflammation. BMC Genomics. 13:377. Published 2012 Aug 6. doi:10.1186/1471-2164-13-377.

Bandsma, R.H.J., Sadiq, K., Bhutta, Z.A., 2019. Persistent diarrhoea: current knowledge and novel concepts. Paediatr. Int. Child. Health. 39 (1), 41–47. https://doi.org/10.1080/20469047.2018.1504412.

Ben-Shachar, S., Yanai, H., Baram, L., Elad, H., Meirovithz, E., Ofer, A., Brazowski, E., Tulchinsky, H., Pasmanik-Chor, M., Dotan, I., 2013. Gene expression profiles of ileal inflammatory bowel disease correlate with disease phenotype and advance understanding of its immunopathogenesis. Inflamm. Bowel Dis. 19 (12), 2509–2521. https://doi.org/10.1097/01.MIB.0000437045.26036.00.

Broadhurst, M.J., Ardeshir, A., Kanwar, B., Mirpuri, J., Gundra, U.M., Leung, J.M., Wiens, K.E., Vujkovic-Cvijin, I., Kim, C.C., Yarovinsky, F., Lerche, N.W., McCune, J. M., Loke, P'ng, Douek, D.C., 2012. Therapeutic helminth infection of macaques with idiopathic chronic diarrhea alters the inflammatory signature and mucosal microbiota of the colon. PLoS Pathog. 8 (11), e1003000. https://doi.org/10.1371/journal.ppat.1003000.

Checkley, W., Buckley, G., Gilman, R.H., et al., 2008. Multi-country analysis of the effects of diarrhoea on childhood stunting. Int J Epidemiol. 37(4):816-830. doi:10.1093/ije/dyn099.

Czarnewski, P., Parigi, S.M., Sorini, C., et al., 2019. Conserved transcriptomic profile between mouse and human colitis allows unsupervised patient stratification. Nat Commun. 10(1):2892. Published 2019 Jun 28. doi:10.1038/s41467-019-10769-x.

Rhesus Macaque Genome Sequencing and Analysis Consortium, Gibbs RA, Rogers J, et al. 2007. Evolutionary and biomedical insights from the rhesus macaque genome. Science. 316(5822):222-234. doi:10.1126/science.1139247.

Gu, Z., Eils, R., Schlesner, M., 2016. Complex heatmaps reveal patterns and correlations in multidimensional genomic data. Bioinformatics 32 (18), 2847–2849. https://doi.org/10.1093/bioinformatics/btw313.

Guarino, A., Ashkenazi, S., Gendrel, D., et al., 2014. European Society for Pediatric Gastroenterology, Hepatology, and Nutrition/European Society for Pediatric Infectious Diseases evidence-based guidelines for the management of acute gastroenteritis in children in Europe: update 2014. J Pediatr Gastroenterol Nutr. 59 (1):132-152. doi:10.1097/MPG.0000000000000375.

Haertel, A.J., Prongay, K., Gao, L., Gottlieb, D.H., Park, B., 2018. Standard growth and diarrhea-associated growth faltering in captive infant rhesus macaques (*Macaca mulatta*). Am. J. Primatol. 80 (9), e22923. https://doi.org/10.1002/ajp.22923.

Holgersen, K., Kutlu, B., Fox, B., et al., 2015. High-resolution gene expression profiling using RNA sequencing in patients with inflammatory bowel disease and in mouse models of colitis. J Crohns Colitis. 9(6):492-506. doi:10.1093/ecco-jcc/jjv050.

Hong, S.N., Joung, J.G., Bae, J.S., et al., 2017. RNA-seq reveals transcriptomic differences in inflamed and noninflamed intestinal mucosa of Crohn's disease patients compared with normal mucosa of healthy controls. Inflamm. Bowel Dis. 23 (7), 1098–1108. https://doi.org/10.1097/MIB.0000000000001066.

Horton, N., Wu, X., Philpott, J., Garber, A., Achkar, J.-P., Brzezinski, A., Lashner, B.A., Shen, B.o., 2016. Impact of low immunoglobulin G levels on disease outcomes in patients with inflammatory bowel diseases. Dig. Dis. Sci. 61 (11), 3270–3277. https://doi.org/10.1007/s10620-016-4294-z.

Horton, N., Kochhar, G., Patel, K., Lopez, R., Shen, B., 2017. Efficacy and factors associated with treatment response of intravenous immunoglobulin in inpatients with refractory inflammatory bowel diseases. Inflamm. Bowel Dis. 23 (7), 1080–1087. https://doi.org/10.1097/MIB.0000000000001116.

Jeong, D.Y., Kim, S., Son, M.J., Son, C.Y., Kim, J.Y., Kronbichler, A., Lee, K.H., Shin, J.I., 2019. Induction and maintenance treatment of inflammatory bowel disease: a comprehensive review. Autoimmun. Rev. 18 (5), 439–454. https://doi.org/10.1016/j.autrev.2019.03.002.

Kim, D., Langmead, B., Salzberg, S.L., 2015. HISAT: a fast spliced aligner with low memory requirements. Nat. Methods 12 (4), 357–360. https://doi.org/10.1038/nmeth.3317.

Lan, Y., Wang, J., Yang, Q., et al., 2020. Blood transcriptome analysis reveals gene expression features of breast-feeding rhesus macaque (*Macaca mulatta*) infants. Zool. Res. 41 (4), 431–436. https://doi.org/10.24272/j.issn.2095-8137.2020.044.

Love, M.I., Huber, W., Anders, S., 2014. Moderated estimation of fold change and dispersion for RNA-seq data with DESeq2. Genome Biol. 15 (12), 550. https://doi.org/10.1186/s13059-014-0550-8.

Magyari, L., Kovesdi, E., Sarlos, P., Javorhazy, A., Sumegi, K., Melegh, B., 2014. Interleukin and interleukin receptor gene polymorphisms in inflammatory bowel diseases susceptibility. World J. Gastroenterol. 20 (12), 3208–3222. https://doi.org/10.3748/wjg.v20.i12.3208.

Merkley, S.A., Beaulieu, D.B., Horst, S., Duley, C., Annis, K., Nohl, A., Schwartz, D.A., 2015. Use of intravenous immunoglobulin for patients with inflammatory bowel disease with contraindications or who are unresponsive to conventional treatments. Inflamm. Bowel Dis. 21 (8), 1854–1859. https://doi.org/10.1097/MIB.0000000000000456.

Moschen, A.R., Tilg, H., Raine, T., 2019. IL-12, IL-23 and IL-17 in IBD: immunobiology and therapeutic targeting. Nat. Rev. Gastroenterol. Hepatol. 16 (3), 185–196. https://doi.org/10.1038/s41575-018-0084-8.

Noble, C.L., Abbas, A.R., Cornelius, J., Lees, C.W., Ho, G.-T., Toy, K., Modrusan, Z., Pal, N., Zhong, F., Chalasani, S., Clark, H., Arnott, I.D., Penman, I.D., Satsangi, J., Diehl, L., 2008. Regional variation in gene expression in the healthy colon is dysregulated in ulcerative colitis. Gut 57 (10), 1398–1405. https://doi.org/10.1136/gut.2008.148395.

Ohkuro, M., Kim, J.-D., Kuboi, Y., Hayashi, Y., Mizukami, H., Kobayashi-Kuramochi, H., Muramoto, K., Shirato, M., Michikawa-Tanaka, F., Moriya, J., Kozaki, T., Takase, K., Chiba, K., Agarwala, K.L., Kimura, T., Kotake, M., Kawahara, T., Yoneda, N., Hirota, S., Azuma, H., Ozasa-Komura, N., Ohashi, Y., Muratani, M., Kimura, K., Hishinuma, I., Fukamizu, A., 2018. Calreticulin and integrin alpha dissociation induces anti-inflammatory programming in animal models of inflammatory bowel disease. Nat. Commun. 9 (1) https://doi.org/10.1038/s41467-018-04420-4.

Oksi, J., Anttila, V.J., Mattila, E., 2019. Treatment of Clostridioides (Clostridium) difficile infection. Ann. Med. 52 (1–2), 1–17. https://doi.org/10.1080/07853890.2019.1701703.

Ostrowski, J., Dabrowska, M., Lazowska, I., et al., 2019. Redefining the Practical Utility of Blood Transcriptome Biomarkers in Inflammatory Bowel Diseases. J Crohns Colitis. 13(5):626-633. doi:10.1093/ecco-jcc/jjy205.

Patel, R.K., Jain, M., Liu, Z., 2012. NGS QC Toolkit: a toolkit for quality control of next generation sequencing data. PLoS One. 7 (2), e30619. https://doi.org/10.1371/journal.pone.0030619.

Pertea, M., Pertea, G.M., Antonescu, C.M., Chang, T.C., Mendell, J.T., Salzberg, S.L., 2015. StringTie enables improved reconstruction of a transcriptome from RNA-seq reads. Nat. Biotechnol. 33 (3), 290–295. https://doi.org/10.1038/nbt.3122.

Pizarro, T.T., Michie, M.H., Bentz, M., et al., 1999. IL-18, a novel immunoregulatory cytokine, is up-regulated in Crohn's disease: expression and localization in intestinal mucosal cells. J. Immunol. 162 (11), 6829–6835.

Planell, N., Masamunt, M.C., Leal, R.F., et al., 2017. Usefulness of Transcriptional Blood Biomarkers as a Non-invasive Surrogate Marker of Mucosal Healing and Endoscopic Response in Ulcerative Colitis. J Crohns Colitis. 11(11):1335-1346. doi:10.1093/ecco-jcc/jjx091.

Planell, N., Lozano, J.J., Mora-Buch, R., Masamunt, M.C., Jimeno, M., Ordás, I., Esteller, M., Ricart, E., Piqué, J.M., Panés, J., Salas, A., 2013. Transcriptional analysis of the intestinal mucosa of patients with ulcerative colitis in remission reveals lasting epithelial cell alterations. Gut 62 (7), 967–976. https://doi.org/10.1136/gutjnl-2012-303333.

Prongay, K., Park, B., Murphy, S.J., 2013. Risk factor analysis may provide clues to diarrhea prevention in outdoor-housed rhesus macaques (*Macaca mulatta*). Am. J. Primatol. 75 (8), 872–882. https://doi.org/10.1002/ajp.22150.

Quraishi, M.N., Acharjee, A., Beggs, A.D., et al., 2020. A Pilot Integrative Analysis of Colonic Gene Expression, Gut Microbiota, and Immune Infiltration in Primary Sclerosing Cholangitis-Inflammatory Bowel Disease: Association of Disease With Bile Acid Pathways. J Crohns Colitis. 14(7):935-947. doi:10.1093/ecco-jcc/jjaa021.

Rai, T., Wu, X., Shen, B., 2015. Frequency and risk factors of low immunoglobulin levels in patients with inflammatory bowel disease. Gastroenterol Rep. (Oxf). 3 (2), 115–121. https://doi.org/10.1093/gastro/gou082.

Rankin, C.R., Theodorou, E., Man Law, I.K., Rowe, L., Kokkotou, E., Pekow, J., Wang, J., Martín, M.G., Pothoulakis, C., Padua, D., 2018. Identification of novel mRNAs and lncRNAs associated with mouse experimental colitis and human inflammatory bowel disease. Am. J. Physiol. Gastrointest Liver Physiol. 315 (5), G722–G733. https://doi.org/10.1152/ajpgi.00077.2018.

Raudvere, U., Kolberg, L., Kuzmin, I., et al., 2019. g:Profiler: a web server for functional enrichment analysis and conversions of gene lists (2019 update). Nucleic Acids Res. 47(W1):W191-W198. doi:10.1093/nar/gkz369.

Rhoades, N., Barr, T., Hendrickson, S., et al., 2019. Maturation of the infant rhesus macaque gut microbiome and its role in the development of diarrheal disease. Genome Biol. 20(1):173. Published 2019 Aug 26. doi:10.1186/s13059-019-1789-x.

Rogosnitzky, M., Danks, R., Holt, D., 2012. Intravenous immunoglobulin for the treatment of Crohn's disease. Autoimmun. Rev. 12 (2), 275–280. https://doi.org/10.1016/j.autrev.2012.04.006.

Shankar, S., Rosenbaum, J., 2020. Chronic diarrhoea in children: a practical algorithm-based approach. J. Paediatr. Child Health. 56 (7), 1029–1038. https://doi.org/10.1111/jpc.14986.

Simats, A., García-Berrocoso, T., Penalba, A., et al., 2018. CCL23: a new CC chemokine involved in human brain damage. J. Int. Med. 283 (5), 461–475. https://doi.org/10.1111/joim.12738.

Su, Y., Zhao, H., 2020. Predisposition of inflammatory bowel disease is influenced by IL-8, IL-10, and IL-18 polymorphisms: a meta-analysis. Int. Arch. Allergy Immunol. 181 (10), 799–806. https://doi.org/10.1159/000509110.

Taman, H., Fenton, C.G., Hensel, I.V., Anderssen, E., Florholmen, J., Paulssen, R.H., 2018. Transcriptomic landscape of treatment-naïve ulcerative colitis. J. Crohns Colitis. 12 (3), 327–336. https://doi.org/10.1093/ecco-jcc/jjx139.

Tang, R., Wang, J., Zhou, M., Lan, Y., Jiang, L., Price, M., Yue, B., Li, D., Fan, Z., 2020. Comprehensive analysis of lncRNA and mRNA expression changes in Tibetan chicken lung tissue between three developmental stages. Anim. Genet. 51 (5), 731–740. https://doi.org/10.1111/age.v51.510.1111/age.12990.

te Velde, A.A., de Kort, F., Sterrenburg, E., Pronk, I., ten Kate, F.J.W., Hommes, D.W., van Deventer, S.J.H., 2007. Comparative analysis of colonic gene expression of three experimental colitis models mimicking inflammatory bowel disease. Inflamm. Bowel Dis. 13 (3), 325–330. https://doi.org/10.1002/ibd.20079.

Tormo, R., Polanco, I., Salazar-Lindo, E., Goulet, O., 2008. Acute infectious diarrhoea in children: new insights in antisecretory treatment with racecadotril. Acta Paediatr. 97 (8), 1008–1015. https://doi.org/10.1111/j.1651-2227.2008.00830.x.

Troeger, C., Blacker, B.F., Khalil, I.A., Rao, P.C., Cao, S., Zimsen, S.RM., Albertson, S.B., Stanaway, J.D., Deshpande, A., Abebe, Z., Alvis-Guzman, N., Amare, A.T., Asgedom, S.W., Anteneh, Z.A., Antonio, C.A.T., Aremu, O., Asfaw, E.T., Atey, T.M., Atique, S., Avokpaho, E.F.G.A., Awasthi, A., Ayele, H.T., Barac, A., Barreto, M.L., Bassat, Q., Belay, S.A., Bensenor, I.M., Bhutta, Z.A., Bijani, A., Bizuneh, H., Castañeda-Orjuela, C.A., Dadi, A.F., Dandona, L., Dandona, R., Do, H.P., Dubey, M., Dubljanin, E., Edessa, D., Endries, A.Y., Eshrati, B., Farag, T., Feyissa, G.T., Foreman, K.J., Forouzanfar, M.H., Fullman, N., Gething, P.W., Gishu, M.D., Godwin, W.W., Gugnani, H.C., Gupta, R., Hailu, G.B., Hassen, H.Y., Hibstu, D.T., Ilesanmi, O.S., Jonas, J.B., Kahsay, A., Kang, G., Kasaeian, A., Khader, Y.S., Khalil, I. A., Khan, E.A., Khan, M.A., Khang, Y.-H., Kissoon, N., Kochhar, S., Kotloff, K.L., Koyanagi, A.i., Kumar, G.A., Magdy Abd El Razek, H., Malekzadeh, R., Malta, D.C., Mehata, S., Mendoza, W., Mengistu, D.T., Menota, B.G., Mezgebe, H.B., Mlashu, F. W., Murthy, S., Naik, G.A., Nguyen, C.T., Nguyen, T.H., Ningrum, D.N.A., Ogbo, F. A., Olagunju, A.T., Paudel, D., Platts-Mills, J.A., Qorbani, M., Rafay, A., Rai, R.K., Rana, S.M., Ranabhat, C.L., Rasella, D., Ray, S.E., Reis, C., Renzaho, A.MN., Rezai, M.S., Ruhago, G.M., Safiri, S., Salomon, J.A., Sanabria, J.R., Sartorius, B., Sawhney, M., Sepanlou, S.G., Shigematsu, M., Sisay, M., Somayaji, R., Sreeramareddy, C.T., Sykes, B.L., Taffere, G.R., Topor-Madry, R., Tran, B.X., Tuem, K.B., Ukwaja, K.N., Vollset, S.E., Walson, J.L., Weaver, M.R., Weldegwergs, K. G., Werdecker, A., Workicho, A., Yenesew, M., Yirsaw, B.D., Yonemoto, N., El Sayed Zaki, M., Vos, T., Lim, S.S., Naghavi, M., Murray, C.JL., Mokdad, A.H., Hay, S.I., Reiner, R.C., 2018. Estimates of the global, regional, and national morbidity, mortality, and aetiologies of diarrhoea in 195 countries: a systematic analysis for the Global Burden of Disease Study 2016. Lancet Infect Dis. 18 (11), 1211–1228. https://doi.org/10.1016/S1473-3099(18)30362-1.

Wang, K.-Y., Christe, K.L., Yee, J.A., Roberts, J.A., Ardeshir, A., 2019. Rotavirus is associated with decompensated diarrhea among young rhesus macaques (*Macaca mulatta*). Am. J. Primatol. 81 (1), e22948. https://doi.org/10.1002/ajp.22948.

Wędrychowicz, A., Zając, A., Tomasik, P., 2016. Advances in nutritional therapy in inflammatory bowel diseases: review. World J. Gastroenterol. 22 (3), 1045–1066. https://doi.org/10.3748/wjg.v22.i3.1045.

Westreich, S.T., Ardeshir, A., Alkan, Z., Kable, M.E., Korf, I., Lemay, D.G., 2019. Fecal metatranscriptomics of macaques with idiopathic chronic diarrhea reveals altered mucin degradation and fucose utilization. Microbiome. 7(1):41. Published 2019 Mar 18. doi:10.1186/s40168-019-0664-z.

WHO, 2017: https://www.who.int/news-room/fact-sheets/detail/diarrhoeal-disease.

Wickham, H., 2106. ggplot2: Elegant Graphics for Data Analysis. Springer-Verlag New York, ISBN 978-3-319-24277-4. doi:10.1007/978-3-319-24277-4.

Williams, M.A., O'Callaghan, A., Corr, S.C., 2019. IL-33 and IL-18 in inflammatory bowel disease etiology and microbial interactions. Front Immunol. 10 (1091) https://doi.org/10.3389/fimmu.2019.01091. Published 2019 May 14.

Wu, F., Dassopoulos, T., Cope, L., et al., 2007. Genome-wide gene expression differences in Crohn's disease and ulcerative colitis from endoscopic pinch biopsies: insights into distinctive pathogenesis. Inflamm. Bowel Dis. 13 (7), 807–821. https://doi.org/10.1002/ibd.20110.

Zhou, M., Zhang, L., Yang, Q., Yan, C., Jiang, P., Lan, Y., Wang, J., Tang, R., He, M., Lei, G., Sun, P., Su, N.a., Price, M., Li, J., Lin, F., Yue, B., Fan, Z., 2020. Age-related gene expression and DNA methylation changes in rhesus macaque. Genomics 112 (6), 5147–5156. https://doi.org/10.1016/j.ygeno.2020.09.021.